

A lattice model approach to the uniaxial behaviour of Textile Reinforced Concrete

J. Hartig, U. Häußler-Combe & K. Schicktanz

Institute of Concrete Structures, Technische Universität Dresden, Dresden, Germany

ABSTRACT: In this contribution, a lattice model for the simulation of the load-carrying and the failure behaviour of Textile Reinforced Concrete (TRC) under monotonic and cyclic tensile loading is presented. A special property of the mentioned composite TRC is that the reinforcement consists of heterogeneous multi-filament yarns of alkali-resistant glass, which are not fully penetrated with matrix of fine-grained concrete. This leads to complex bond conditions. The lattice model for the simulation consists of one-dimensional strands of bar elements with limited tensile strength, which represent the matrix as well as the reinforcement. These strands are connected with zero-thickness bond elements, which use non-linear bond laws as element characteristics. These bond laws contain a damage algorithm to include a possible degradation of the bond quality due to mechanical loading. This nonlinear problem is solved within a Finite Element Method formulation. Simulations of tensile specimens are performed and compared to experimental data for both monotonic and cyclic loading.

1 INTRODUCTION

Concerning the strengthening and retrofitting of existing steel-reinforced concrete structures built during the last century it is often desirable to apply additional thin load-carrying layers. A possible approach, which offers these properties are layers of Textile Reinforced Concrete (TRC) (Hegger 2001; Curbach 2003; Hegger et al. 2006; Brameshuber 2006). This material is a composite of textile-processed yarns of endless fibres as reinforcement and a fine-grained concrete as matrix. In this context fine-grained means a much smaller maximum aggregate size, e.g. 1 mm, than used for normal concrete. Textiles produced of yarns, made of glass filaments or carbon filaments, are typically embedded in the concrete matrix. Usually yarns of glass, which have to be alkali-resistant to sustain long-term embedded in the concrete (Schorn & Schiekel 2004), consist of up to 2000 filaments with diameters of 10-30 microns.

Unlike Fibre Reinforced Plastics (FRP), the yarns are not fully penetrated with matrix, because the empty spaces in the filament bundles are too narrow for the particles of the cement paste. Hence, there can be found two different bond zones inside a yarn. In the sleeve zone of the yarn where the filaments contact the matrix adhesional bond is dominating. Supposedly, the load transfer properties of the interface between the matrix and the filaments are load dependent, which can result in damage of the bond at higher load levels. Almost no cement paste intrudes into the

core zone. Hence, only a frictional load transfer at the contact areas of the filaments is possible. Additionally, the concrete as well as the filaments have a limited tensile strength, which leads to a crack development in the concrete and the failure of filaments or whole yarns. Altogether, even under monotonic tensile loading a complex structural behaviour is observable.

A lattice approach is developed to simulate the above-mentioned properties. Because only pure tensile loads are regarded, the model has only degrees of freedom in the load direction, which is called the longitudinal direction in the following. The whole concrete component is considered as homogeneous. Thus, it can be modelled as a serial connexion of elements. The yarn consisting of several filaments not fully penetrated with cement slurry, as mentioned above, cannot be assumed homogeneous. While the longitudinal direction is also modelled as a serial connexion of elements, the transverse direction is regarded by splitting the yarn component into a number of segments, which are also assumed to be homogeneous. These segments are regularly arranged in a lattice scheme. Among themselves, the segments are coupled with zero-thickness bond elements, which act nonlinear according to bond laws. The adhesional bond between the concrete and the filaments is subject to damage, which is applied to the bond law to ensure a proper description of the behaviour. For the core segments, which underlie only a frictional bond, a constant bond stress is assumed. Besides that, lim-

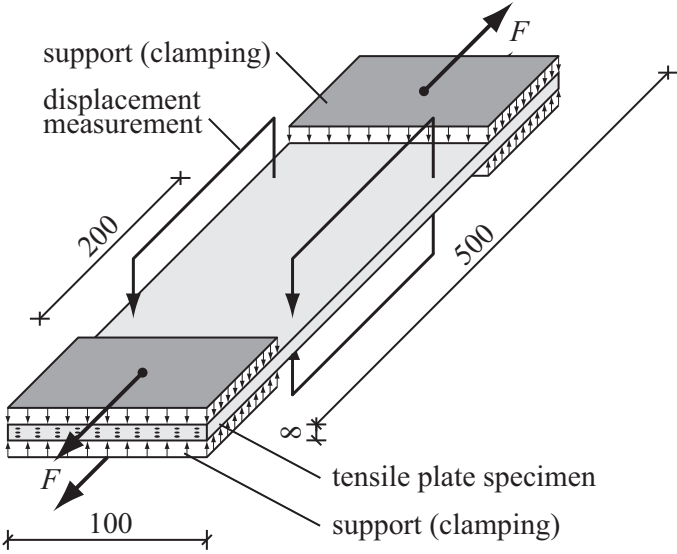


Figure 1. Typical specimen and test setup used by (Jesse 2004) for tensile tests on TRC (dimensions in mm)

ited tensile strength is applied to the elements with the consequence of propagating cracks. This highly nonlinear problem is solved with a Finite Element Method formulation. The model is able to reproduce the results of experiments performed under both monotonic and cyclic tensile loading, as for example experiments with unidirectional reinforced tensile specimens. Thus, experimental results are used to verify the computational results and to identify possible weaknesses of the model.

2 EXPERIMENTAL OBSERVATIONS

Textile Reinforced Concrete has a tensile structural behaviour, which is in principle comparable with other continuously reinforced composites as for instance steel rebar reinforced concrete. The used multi-filament reinforcement has to bear the tensile forces after the concrete cracking. The concrete matrix has to transfer the external tensile loads to the reinforcement and has to carry compressive loads. Special characteristics regarding the load-carrying behaviour arise from the heterogeneous constitution of the multi-filament yarns. It is for example observable that the mean strength of a yarn is lower than the mean strength of a single filament (Abdkader 2004). A number of reasons are responsible for this behaviour as for instance statistical effects (Daniels 1944), unequal loading of the filaments in a yarn (Chudoba et al. 2006; Vořechovský & Chudoba 2006) or damaging of the yarns and filaments in the production and treatment processes (Abdkader 2004).

For the investigation of the structural behaviour of composites under uniaxial loading tensile specimens are often used. For the case of Textile Reinforced Concrete such investigations were made for

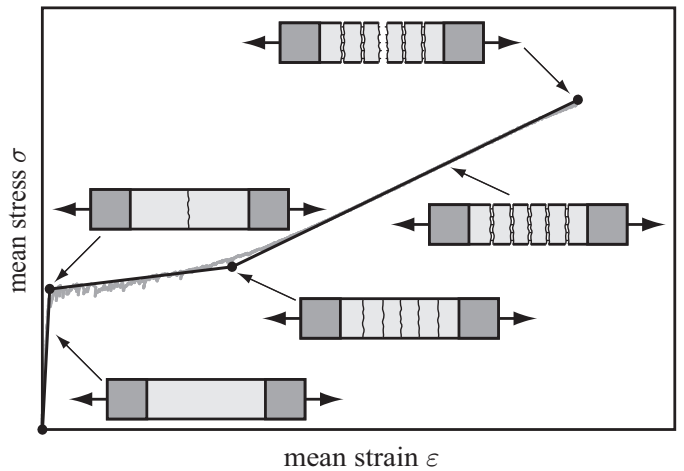


Figure 2. Typical stress-strain relation and associated crack patterns for tensile specimens under monotonic loading as shown in Figure 1

example by (Jesse 2004; Curbach 2003) and (Molter 2005), which show similar results. Hence, only a subset of JESSE's comprehensive experimental data will be discussed here. In (Jesse 2004) results of specimens investigated under monotonic tensile loading are published. Besides these tests, JESSE made also experiments under cyclic loading, which are hitherto unpublished. The specimens under consideration are unidirectional reinforced with yarns of alkali-resistant glass with reinforcement ratios varying between 1–3 Vol. %.

In Figure 1, a typical specimen used by JESSE is shown with its dimensions. During the test, the specimen is fixed in a hydraulic testing machine with clamping devices as indicated in Figure 1 as well. The tensile loads are applied displacement-controlled with a rate of about 0.015 mm/s. On a length of 200 mm, the longitudinal displacements are measured on both sides of the specimen, see Figure 1. In Figure 2, a typical stress-strain relation is shown where the measured forces F are related to the specimens cross-sectional area leading to a mean stress σ and the measured displacements are related to the measurement length leading to a mean strain ε .

The stress-strain relation starts with a linear increase, principally according to the Young's modulus of the concrete, until the tensile strength of the concrete is reached and the matrix cracks for the first time. Upon this point, the yarn reinforcement has to bear the applied tensile load at the crack. If a sufficient amount of reinforcement with an ample bond capacity is available, further cracks will develop under increasing external tensile load. In the following part of the stress-strain relation, this is associated with a decreased slope of the curve (Figure 2). The crack development in the concrete continues until the load transferred from the reinforcement to the matrix between two cracks is too low to reach the tensile strength of the concrete again. If the final crack

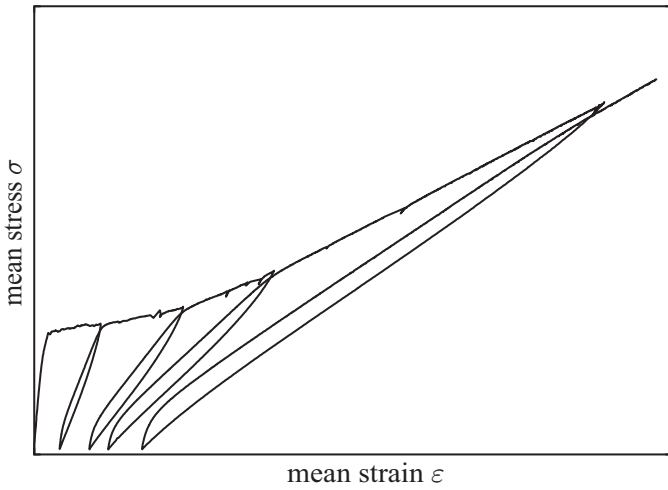


Figure 3. Typical experimental stress-strain relation under cyclic loading for tensile specimens as shown in Figure 1

pattern is reached, the stress-strain relation increases again until the tensile strength of the reinforcement is reached too and the specimen finally fails, often in a brittle manner. The slope of the stress-strain relation in this state is mostly influenced by the properties of the reinforcement. Nevertheless, the concrete participates of course in the load-carrying between the cracks, which is well-known as tension stiffening.

In the case of cyclic loading, the stress-strain relation of the monotonic loading case can be seen as the envelope of the cyclic relation. The observed unloading paths of the stress-strain relation are Z-shaped. This means that the stress-strain relation decreases according to a steeper slope compared with the loading path. In the middle part of the unloading path, the slope becomes flatter and the stress-strain relation decreases almost linearly. Near the abscissa the slope of the stress-strain relation increases again. This increase of the stiffness can probably be explained with a compressional reloading of the concrete. It is also observable that during the unloading the origin is not reached again. This effect can be considered as a macroscopic plastic deformation. With reaching higher load levels the plastic deformation also increases. The increase of the plastic deformation is more pronounced in the cracking state than in post-cracking state, which can be caused by an initial stressless deformation of the reinforcement at the cracks. The mean slopes of the unloading paths are steeper at lower load levels than at higher ones. The reloading is characterised by a steep increase of the stress-strain relation, which passes into a flatter linear slope and merges into the envelope curve. The mean slopes of the reloading paths are also steeper at lower load levels than at higher load levels. According to the envelope curve, also the cyclic loaded specimen finally fails reaching the tensile strength of the reinforcement.

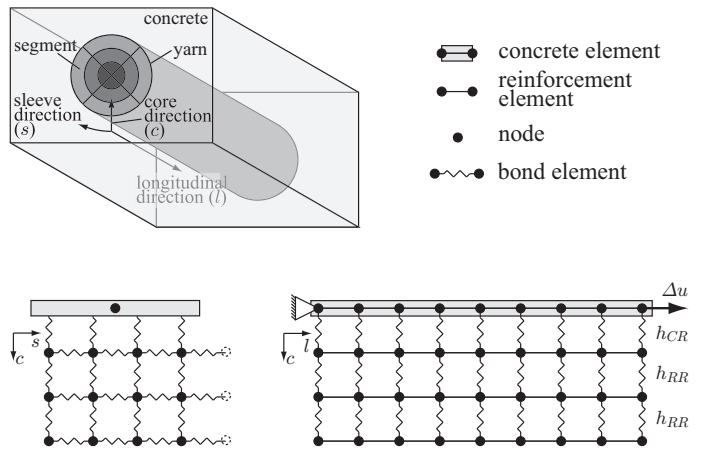


Figure 4. Geometrical model (top) and lattice discretisation in the cross section (bottom left) and the longitudinal section (bottom right)

3 MODELLING

3.1 Mechanical model

In the following, a lattice model used for the determination of the structural behaviour of Textile Reinforced Concrete will be described, which was partly developed in previous contributions. In (Häußler-Combe & Hartig 2006a) a one-dimensional mechanical model for the determination of the load-bearing and the failure behaviour of Textile Reinforced Concrete was developed. This model was enhanced in (Häußler-Combe & Hartig 2006b) with a bond law using a damage algorithm to include the degradation of the bond quality between concrete and reinforcement.

The model is in principle a combination of strands of bar elements for the constituents of the composite, which are each assumed to be homogeneous. The concrete as well as the reinforcement elements have prescribed limited tensile strengths, which can lead to cracking while loading. The strands are connected at the nodes with zero-thickness bond elements, which act according to bond laws. The heterogeneity of the reinforcement is considered by segmentation into several strands as it is shown in principle in Figure 4. The segments are arranged in a lattice scheme, which simplifies the computational implementation. Depending on the resolution, in one segment several filaments or yarns are pooled, which are assumed to be homogeneous with effective material properties.

As mentioned before, the bond elements act according to bond laws formulated as bond stress-slip relations. Experimental investigations for the determination of the bond properties between single filaments and concrete were made for instance by (Banhözer 2004) and (Zhendarov & Mäder 2005). Such experimental results are used to estimate the magnitude of the bond force, but are not directly applicable for bond laws of a whole yarn or parts of it. The bond stress-

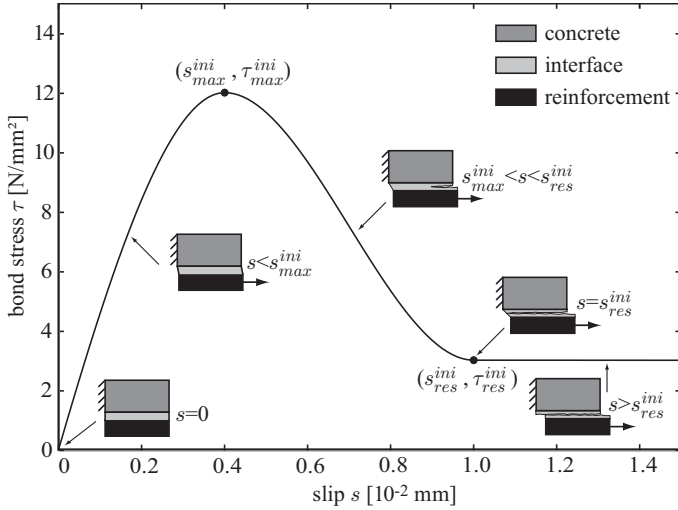


Figure 5. Bond stress-slip relation h_{CR} for the case of concrete-sleeve interaction in the initial state

slip relation h_{CR} used in the model for the interaction between the concrete and the sleeve segments is shown in Figure 5 in its initial state. The bond law implements a combination of damage and plasticity to take into account bond degradation due to loading. The algorithm for the degradation evolution of the bond stress is schematically shown in Figure 6 using an arbitrarily chosen loading path. Figure 6 includes also the state diagram with the starting point (●) of the algorithm and all possible state transitions. The numbers of the states in the state diagram correspond to those in the bond stress-slip relation.

The bond law h_{CR} for the concrete-sleeve interaction starts with an increase until the maximum value of the bond stress τ_{max}^{ini} corresponding to the slip s_{max}^{ini} is reached. This peak point is the maximum possible value of bond stress that can be transferred. After this peak, the bond stress-slip relation decreases until the residual bond stress τ_{res}^{ini} corresponding to the slip s_{res}^{ini} is reached. With larger slip values than s_{res}^{ini} only a frictional load transfer is assumed with a bond stress value τ_{res} . This bond stress value can be kept constant or can further decrease with increasing slip.

If a slip reduction occurs after the peak point in the softening state 1 (Figure 6), where the bond is degraded to a certain amount, the initial maximum bond stress necessarily cannot be reached again. A reduction of the slip value can occur for instance due to cracking resulting in a local stress relocation. An unloading path (state 3) different from the loading path (state 0) is used in the bond law h_{CR} to avoid a trace back to the initial peak. Therefore, the bond stress $\tau_{max}^{act,1}$ corresponding to the currently largest reached slip $s_{max}^{act,1}$ is stored and used as new maximum value $\tau_{max}^{act,1}$. The unloading path (state $3^{(1)}$) is modelled as linear decrease of the bond stress and the slip according to the slope between the origin of the coordinate system and the initial peak point ($s_{max}^{ini}, \tau_{max}^{ini}$). The value of the bond stress is limited to the negative abso-

lute value of the currently largest bond stress $-\tau_{max}^{act,1}$. This point is reached with the chosen load path in Figure 6 via the state $3^{(1)}$ and the state $4^{(1)}$. A further reduction of the slip will decrease the absolute maximum bond stress value, which is the case in Figure 6 where the slip decreases to $s_{max}^{act,2'}$ with the corresponding bond stress $-\tau_{max}^{act,2'}$. At this point, the load in association with the slip as well as the bond stress increase again (Figure 6). Thus, the state 1 will be reached again via the states $4^{(2)}$ and $3^{(2)}$. While the slip in state 1 further increases, the bond stress decreases until the residual bond stress τ_{res}^{ini} is reached, which is equivalent with a purely frictional load transfer.

For the interaction between the sleeve and the core zone of a yarn pure friction is assumed. The corresponding bond law h_{RR} is in principle the same as h_{RR} but has no peak value τ_{max}^{ini} at s_{max}^{ini} . A constant bond stress of 3 N/mm^2 for both τ_{max}^{ini} and τ_{res}^{ini} is assumed.

The interpolation between the supporting points of the bond stress-slip relations can be performed according to several approaches. A multi-linear approach is used for example by (Richter & Zastrau 2006) in conjunction with an analytical modelling approach. In numerical simulations, the discontinuities of the derivatives on the transition between the intervals of the multi-linear relations lead possibly to numerical problems during computations. This can be avoided using special cubic polynomials, which show monotonicity and continuity in the first derivatives between consecutive intervals. As underlying algorithm, the Cubic Hermite Interpolating Polynomial Procedure (PCHIP) by (Fritsch & Carlson 1980), which is also published in (Kahaner et al. 1989), is used. It ensures a smooth, shape preserving interpolation of the bond stress-slip relation given by a number of data points without producing additional bumpiness or oscillations as it could be the case for example with a spline interpolation (de Boor 1978). As supporting points for the bond law h_{CR} (Figure 5) the origin of the coordinate system, the peak point, the residual point and an end point are used.

3.2 Numerical model

The lattice model presented in the previous section is the basis for a numerical model formulated within the Finite Element Method (FEM). In longitudinal direction, the concrete and the yarn strand are discretised with one-dimensional bar elements of a length of 0.1 mm . This leads with the specimen length of 500 mm (Figure 1) to 5000 elements per segment strand. A finer discretisation does not affect the results significantly, whereas coarser discretisations cannot approximate the used bond law in a sufficient manner and overestimate the macroscopic stiffness of a crack bridge. The boundary conditions are given with

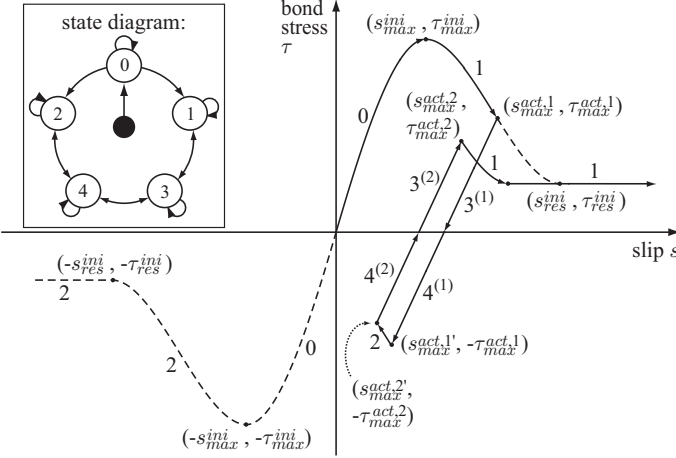


Figure 6. Degradation algorithm implemented in the bond stress-slip relation h_{CR} evolved from an arbitrarily chosen loading

prescribed displacements at the concrete's end nodes. The displacement is zero at $x = 0$ mm and becomes continuously increased at $x = 500$ mm for the case of monotonic loading. For the case of cyclic loading the displacement at $x = 500$ mm is increased and reduced according to a load regime as used in the experiments. As mentioned in the previous section the strands are connected with bond elements, which act according to bond laws also introduced in this section. The free value of the bond law is the slip, which is determined by the difference of the displacements between the two nodes of a bond element.

Besides the nonlinearities resulting from the bond law, additional nonlinearities arise from limited tensile strengths for both the concrete and the reinforcement. To avoid the failure of a series of elements in the case of constant or nearly constant stresses in the longitudinal direction, the failure of elements is limited to one per load step. The bar elements used to represent the concrete in the clamping zones are assumed not to crack on a length of 100 mm from the ends of the specimen to avoid failure at the concrete section's end nodes.

The resulting system of nonlinear equations is solved using the Broyden-Fletcher-Goldfarb-Shanno (BFGS) approach, which is a Quasi-Newton-Method, in combination with a line-search algorithm (Bathe 1996; Matthies & Strang 1979; Nocedal & Wright 1999). Some more details regarding the numerical implementation related to the stated problem are presented in (Häußler-Combe & Hartig 2006a).

4 COMPUTATIONS

4.1 Geometrical and material parameters

So far, the model is specified in principle. For the computations a specialised model is used, which consists of three bar element strands: one strand for the

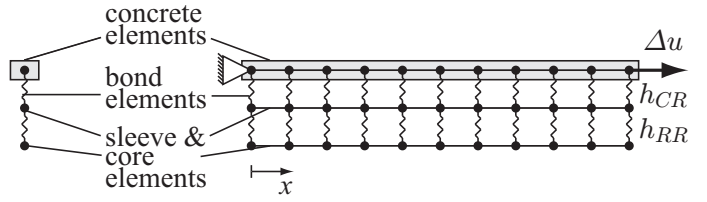


Figure 7. Specialised model with three element strands in the cross section (left) and the longitudinal section (right)

concrete and two strands for the yarn reinforcement, see Figure 7. In this model, the concrete strand is only connected with the so-called sleeve strand via bond elements using the bond law h_{CR} for adhesional bond as element characteristic. The sleeve strand is additionally coupled with the core strand via bond elements acting according to the bond law h_{RR} , which represents purely frictional load transfer.

The tensile strength of the concrete is assumed with 6.5 N/mm² and the Young's modulus is defined with 28,500 N/mm² (Jesse 2004). The cross-sectional area of the concrete of 771 mm² is determined by the width of 99.5 mm and the thickness of 7.8 mm of the specimen. The reduction of the cross-sectional area of the concrete due to the reinforcement is neglected.

The reinforcement material are yarns of alkali-resistant glass with a unit length weight of 310 tex produced by Nippon Electric Glass. The Young's modulus was determined by (Abdkader 2004) with $E_{yarn} = 79,950$ N/mm². The total cross-sectional area of the reinforcement $A_{reinf} = 14.6$ mm² results from the number of yarns $n_{yarn} = 134$ and the cross-sectional area of a yarn $A_{yarn} = 0.11$ mm². Hence, the specimen was reinforced with a ratio of about 1.9 Vol. %. According to the model, the reinforcement is splitted into two parts, the sleeve strand with 25 % of the total cross-sectional reinforcement area and the core strand with 75 % of the total cross-sectional reinforcement area. This ratio is approximated on the base of microscopic observations on transparent cuts of yarns embedded in a cementitious matrix.

The strands of bar elements are coupled with bond elements for which the bond surface areas have to be defined. The bond surface areas S_{sleeve} and S_{core} are assumed to be the lateral surface areas of cylinders, which have the cross-sectional area of a homogeneous yarn A_{yarn} :

$$\begin{aligned} S_{sleeve} &= n_{yarn} \cdot l \cdot C_{yarn} \\ &= n_{yarn} \cdot l \cdot (2\sqrt{\pi A_{yarn}}) \end{aligned} \quad (1)$$

$$\begin{aligned} S_{core} &= n_{yarn} \cdot l \cdot C_{core} \\ &= n_{yarn} \cdot l \cdot (2\sqrt{\pi \cdot 0.75 \cdot A_{yarn}}) \end{aligned} \quad (2)$$

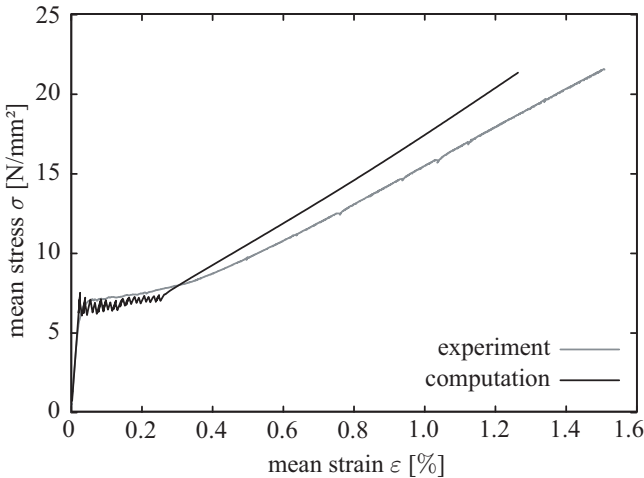


Figure 8. Computational and experimental stress-strain relation for the case of monotonic loading

In these equations l is the element length, C_{yarn} the circumferences of a homogeneous circular yarn and C_{core} of the core fraction of a yarn respectively. In these bond surface areas possible roughness or ellipticity of the yarn boundary is not included, because the bond forces finally result from the product of the bond surface areas and the bond stresses. The tensile strength of the yarns is defined with 1357 N/mm^2 (Abdkader 2004).

4.2 Monotonic loading

In Figure 8 the computed and an experimentally obtained stress-strain relation for the case of monotonic tensile loading is shown. It can be seen that the uncracked state in the simulation coincides with the experimental data. Because the slope of this linear increase is mostly influenced by the Young's modulus of the concrete, this agreement could be expected as well as the transition point to the cracking state, which depends on the tensile strength of the concrete.

The computed mean slope of the cracking state of the concrete also agrees with the experimental data, but the drops of the stress after each concrete crack are larger than observed in the experiments. This results from the as purely brittle implemented failure of the concrete, which is not observable in reality. It is well known that concrete is able to transfer stresses over small cracks to a certain amount, which depends on the crack width. This effect is called tension softening and according to (Brockmann 2006) it also exists in the special kind of concrete used in the experiments under consideration. A further fact, which implies that tension softening would lead to more realistic computational results, is the calculated total number of cracks. It is lower than the number of cracks observed in the experiments.

After the crack development has finished, the computed stress-strain relation increases again, which

agrees with the behaviour in the experiments. However, the computed slope in this state is larger than in the experiments. The reasons for this discrepancy are currently not clear. It can be speculated that a certain number of highly bonded filaments fails prematurely. This has to happen simultaneous with the concrete, because if it would occur after the concrete cracking has finished the slope in the stress-strain relations would have to decrease non-linearly, which is not observable in the experimental data. Another reason could be that de facto a lower number of yarns were inserted in the experiment. A reason, which is currently favoured by the authors, is that some kind of telescopic effect appears due to the heterogeneous structure of the yarns and the non-uniform bond conditions in the yarn. This could be modelled with a finer discretisation of the yarn, which means that more reinforcement strands have to be connected in parallel.

The failure of the whole structure occurs if the tensile strength of firstly the sleeve strand and secondly the core strand of the reinforcement are reached. While a good agreement between the simulation and the experiment regarding the ultimate stress is observable, the ultimate strain is according to the slope of the stress-strain relation in this state lower in the simulation as observed in the experiment.

4.3 Cyclic loading

As mentioned before, with the model it is also possible to simulate the stress-strain behaviour under cyclic loading. Therefore, the model used in the previous section was loaded with four load cycles on different load levels. In Figure 9 the simulated stress-strain relation is compared with an experimental one. The stress-strain relation for the case of monotonic loading can be seen as the envelope for the cyclic stress-strain relation. Thus, the uncracked state, the cracking and the final cracking state are computed with the same quality as described for the case of monotonic loading in the previous section.

The first load cycle was executed in the state of ongoing cracking. The shape of the stress-strain relation in the computed cycle agrees in principle with the experimental observations. After a steep decrease the unloading path becomes flatter. However, the unloading path reaches a lower strain level in the simulations compared with the experiment, which means that the macroscopic observable plastic deformations are underestimated. A reason could be the participation of the concrete on the load-carrying at the cracks while unloading. It can be assumed that the cracks in the concrete do not close perfectly for example due to loosened particles and the relaxation of eigenstresses. Thus, the concrete is locally stressed compressional, which leads to a macroscopic plastic deformation. This effect cannot be reproduced with the

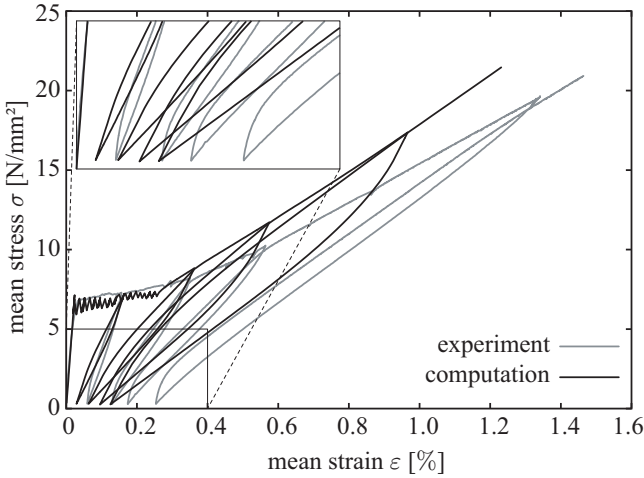


Figure 9. Computational and experimental stress-strain relation for the case of cyclic loading

current model. Another source of possible plastic deformations exists in the unloading path of the bond law described in Section 3.1. The slope of this unloading path in the bond law is currently arbitrarily chosen and is thus open for further improvements.

The shape of the reloading path of the experimental stress-strain relation agrees with the assumption of a moderate compressional pre-stressing of the concrete, because at the beginning of the reloading the stress-strain relation increases according to the Young's modulus of the concrete. This is not observable in the simulated stress-strain relation where the reloading starts with a flatter slope caused by the bond law and the stiffness of the reinforcement. Afterwards, in both the experimental and the simulated stress-strain relation the reloading path merges towards the monotonic stress-strain relation and follows it during further loading.

The other three load cycles are beyond the cracking state in the stress-strain relation, see Figure 9. In all three cycles, the characteristics described for the first cycle are repeated in principle, but the differences between simulation and experiment become more pronounced. Especially the compression of the concrete near the end of the unloading is clearly observable in the last cycle of the experimental data. There as well as in the previous cycles, the unloading path becomes stiffer near the abscissa. As mentioned before, this is not observable in the simulation, because the compression of the concrete after cracking is not implemented in the model. This is also the reason, why the reloading paths in the computed stress-strain relation start always flatter than in the experimentally obtained relation.

In agreement with the experimental data, the cycles on lower load levels behave stiffer than cycles on higher load levels and the hystereses become larger as well. The area in between a hysteresis is a measure of the dissipated energy. Looking on Figure 9 it can be seen that in the simulation too much energy is dis-

sipated compared with the experiments. One reason is the simulated stiffness in the final cracking state, which is larger than in the experiment. This leads to more pronounced hystereses.

Regarding the occurring macroscopic observable plastic deformations, it must be concluded that the model underestimates these deformations. A possible reason is an initial slack, which could lead to a delayed activation of the yarn reinforcement. This could lead to stressless deformations. A fine-tuning of the parameters used in the model basing on a detailed study of several experimental will improve the agreement between the model and the experiment.

5 CONCLUSIONS

The load-carrying and failure behaviour of Textile Reinforced Concrete shows complexity even in the case of purely tensile loading. This behaviour is simulated with a lattice model reduced to the essential. The distinction between matrix and yarn, the different bond zones in the yarn and the limited tensile strength are assessed as essential properties. The spatial material distribution seems in the case of unidirectional reinforcement and loading less important. Hence, the presented model has a one-dimensional geometry but takes material-specific nonlinearities like limited tensile strengths and nonlinear bond laws with damage into account.

The presented computational results are showing a good agreement with the experimental data, although some deficiencies are still existing. A further improvement of the computational results could be reached by the implementation of tension softening for the fine-grained concrete to include the load transmission over a concrete crack and to simulate the crack patterns in the concrete more realistic. However, this will primarily ameliorate the computational results quantitatively. Regarding the cyclic loading, a modification of the unloading path of the bond law can possibly improve the computational results.

An important exercise is the estimation of the parameters used in the simulations. The material parameters for instance the tensile strengths or the Young's moduli of the concrete and the yarns are sufficiently well known but the knowledge about the interaction between matrix and reinforcement is still lacking. It is for example not experimentally confirmed how strong and durable the bond between matrix and reinforcement is. Further investigations are necessary to clarify these open questions.

ACKNOWLEDGEMENT

The authors gratefully acknowledge the financial support of this research from Deutsche Forschungs-

gemeinschaft DFG (German Research Foundation) within the Sonderforschungsbereich 528 (Collaborative Research Center) "Textile Reinforcement for Structural Strengthening and Retrofitting" at Technische Universität Dresden as well as their colleagues for providing the experimental data.

REFERENCES

- Abdkader, A. (2004). *Charakterisierung und Modellierung der Eigenschaften von AR-Glasfilamentgarnen für die Betonbewehrung*. Ph. D. thesis, Technische Universität Dresden, Dresden.
- Banholzer, B. (2004). *Bond behaviour of a Multi-Filament Yarn embedded in a cementitious Matrix*. Ph. D. thesis, RWTH Aachen, Aachen.
- Bathe, K. (1996). *Finite Element Procedures*. Englewood Cliffs, New Jersey: Prentice-Hall.
- Brameshuber, W. (ed.) (2006). *State-of-the Art Report of RILEM Technical Committee 201 TRC: Textile Reinforced Concrete*. RILEM Publications Report 36. Bagnoux: RILEM.
- Brockmann, T. (2006). *Mechanical and fracture mechanical properties of fine grained concrete for textile reinforced composites*. Ph. D. thesis, RWTH Aachen, Aachen.
- Chudoba, R., Vořechovský, M. & Konrad, M. (2006). Stochastic modeling of multi-filament yarns. I. Random properties within the cross-section and size effect. *International Journal of Solids and Structures* 43: 413–434.
- Curbach, M. (ed.) (2003). *Textile Reinforced Structures - Proceedings of the 2nd Colloquium in Textile Reinforced Structures (CTRS2)*, Dresden: TU Dresden.
- Daniels, H. (1944). The statistical theory of the strength of bundles of threads. I. *Proceedings of the Royal Society of London A183*: 405–435.
- de Boor, C. (1978). *A Practical Guide to Splines*. Number 27 in Applied Mathematical Sciences. New York: Springer-Verlag.
- Fritsch, F. & Carlson, R. (1980). Monotone Piecewise Cubic Interpolation. *SIAM Journal on Numerical Analysis* 17(2): 238–246.
- Häußler-Combe, U. & Hartig, J. (2006a). Structural behaviour of textile reinforced concrete. In Meschke, G.; de Borst, R.; Mang, H. & Bicanic, N. (eds), *Computational Modelling of Concrete Structures - Proceedings of the EURO-C 2006, Mayrhofen, 27-30 March 2006*: 863–872. London: Taylor& Francis.
- Häußler-Combe, U. & Hartig, J. (2006b). Uniaxial structural behavior of TRC - A one-dimensional approach considering the transverse direction by segmentation. In Hegger, J.; Brameshuber, W. & Will, N. (eds), *Textile Reinforced Concrete - Proceedings of the 1st International RILEM Symposium, Aachen, 6-7 September 2006*: 203–212. Bagnoux: RILEM.
- Hegger, J. (ed.) (2001). *Textilbeton - 1. Fachkolloquium der Sonderforschungsbereiche 528 und 532*, Aachen: RWTH Aachen.
- Hegger, J.; Brameshuber, W. & Will, N. (eds) (2006). *Textile Reinforced Concrete - Proceedings of the 1st International RILEM Symposium, Aachen*, RILEM Publications PRO 50, Bagnoux: RILEM.
- Jesse, F. (2004). *Tragverhalten von Filamentgarnen in zementgebundener Matrix*. Ph. D. thesis, Technische Universität Dresden, Dresden.
- Kahane, D.; Moler, C. & Nash, S. (1989). *Numerical Methods and Software*. London: Prentice-Hall.
- Matthies, H. & Strang, G. (1979). The solution of non-linear finite element equations. *International Journal for Numerical Methods in Engineering* 14: 1613–1626.
- Molter, M. (2005). *Zum Tragverhalten von textilbewehrtem Beton*. Ph. D. thesis, RWTH Aachen, Aachen.
- Noceodal, J. & Wright, S. (1999). *Numerical Optimization*. Springer Series in Operations Research. New York: Springer-Verlag.
- Richter, M. & Zastraub, B. (2006). On the nonlinear elastic properties of textile reinforced concrete under tensile loading including damage and cracking. *Materials Science and Engineering A* 422: 278–284.
- Schorn, H. & Schiekel, M. (2004). Prediction of lifetime of alkali-resistant glass fibres in cementitious concretes. In di Prisco, M.; Felicetti, R. & Plizzari, G. (eds), *6th RILEM Symposium on Fibre-Reinforced Concretes (FRC) - BEFIB 2004, Volume 1, Varenna, 20-22 September 2004*: 615–624. Bagnoux: RILEM.
- Vořechovský, M. & Chudoba, R. (2006). Stochastic modeling of multi-filament yarns. II. Random properties over the length and size effect. *International Journal of Solids and Structures* 43: 435–458.
- Zhandarov, S. & Mäder, E. (2005). Characterization of fiber/matrix interface strength: applicability of different tests, approaches and parameters. *Composites Science and Technology* 65: 149–160.